ECCOMAS Thematic Conference on Computational Methods
in Structural Dynamics and Earthquake Engineering
M. Papadrakakis, D.C. Charmpis, N.D. Lagaros, Y. Tsompanakis (eds.)
Rethymno, Crete, Greece, 13–16 June 2007

RESPONSE AND RELIABILITY OF NONLINEAR SYSTEMS WITH IMPACTS SUBJECTED TO TRANSIENT EXCITATIONS

Kyriakos Perros[1], Costas Papadimitriou[1], Spyros Karamanos[1], and Panagiotis Panetsos[2]

[1]University of Thessaly
Department of Mechanical & Industrial Engineering, Volos 38334, Greece
kyperros@uth.gr, costasp@uth.gr, skara@uth.gr

[2]Egnatia Odos A.E.
Design Department, 6th Km Thessaloniki-Thermi, P.O. Box 60030, GR-570 01 Thermi, Greece
ppane@egnatia.gr

Keywords: Bridges, Seismic Analysis, Piecewise Linear System, Reliability, Probabilistic Response Spectra

Abstract. *This work investigates the response and reliability of a class of nonlinear elastic and inelastic systems with impacts arising in mechanical and civil engineering applications. The study focuses on civil engineering applications related to bridges equipped with seismic stoppers to resist earthquakes. These systems are represented by structural models with piecewise linear elastic stiffness elements and often involve strong inelastic behavior due to yielding of the piers. In order to gain useful insight into the behavior of these systems, one degree of freedom piecewise linear elastic mechanical models are first analyzed and the behavior to short duration sine pulses as well as longer duration transient and stochastic earthquake excitations is investigated. The analysis is then extended to nonlinear single degree of freedom structural models possessing combined piecewise linear elastic and elasto-plastic restoring force characteristics. The analysis is concentrated on the estimation of the sensitivity of the deterministic and probabilistic response spectra characteristics to system and loading parameters such as stiffness ratio, gap sizes between deck structure and stoppers, inelastic parameters, excitation strength and frequency content. The subset simulation method is used to efficiently estimate the probabilistic response spectra The analysis is then extended to investigate the response and reliability of the four-span Kavala bridge, located in northern Greece. The bridge deck is supported on columns through elastomeric bearings. Seismic stoppers are used, designed to be activated well under the design earthquake level, thus critically contributing to the main earthquake resisting mechanism. A multi degree of freedom finite element models of the bridge, involving piecewise linear stiffness elements, is used to simulate its behavior. Deterministic short duration sine pulse excitations as well as white noise stochastic excitations are used to simulate the earthquake excitations. The sensitivity of the response and failure probability to the size of gaps is explored in order to gain insight on the performance of the bridge structure and the effect of gap sizes.*

1 INTRODUCTION

Nonlinear elastic and inelastic systems with impacts arise in mechanical and civil engineering applications. In mechanical engineering applications, the behavior of the systems with impacts are often analyzed using single or multi degree of freedom mechanical models with piecewise linear elastic stiffness elements [1,2]. The interest concentrates on the response and stability of piecewise linear elastic systems to periodic excitation and it has been shown that these systems manifest complex nonlinear behavior. In civil engineering applications, such systems arise in the analysis of bridges with seismic stoppers [3-5] or the analysis of pounding of adjacent buildings. These systems are represented by single and multi degree of freedom models with piecewise linear elastic stiffness elements that often involve strong inelastic behavior in parts of the system.

The present study focuses on the analysis of bridges that involve impacts due to the seismic stoppers designed to effectively withstand earthquake loads and reduce the size of the piers. A simple bridge with seismic stoppers is shown in Figure 1a. The bridge deck is connected to the piers by elastomeric bearings and seismic stoppers are added on the pier caps that have a small gap with the deck structure so that the elastomeric bearings are free to move under ambient or traffic loads, while they impact on the stoppers only under moderate or strong earthquake loads. Activation of the stoppers due to impact results in sudden increase of the stiffness of the structure. The gaps between the stoppers and the bearings are usually selected such that the impact with the stoppers occurs before the pier yielding. Assuming a heavy undeformed deck of mass M and representing the stiffness of the piers and the elastomeric bearing by massless linear or inelastic springs, one can construct a single degree of freedom (SDOF) simplified model of the bridge as shown in Figure 2a. For the case of stopper activation but no pier yielding, the springs are linear and the simplified system in Figure 2a behaves as a SDOF piecewise linear elastic system. For the case of elastoplastic spring representing the inelastic behavior of the deck, the system in Figure 2a behaves as a SDOF piecewise linear inelastic system.

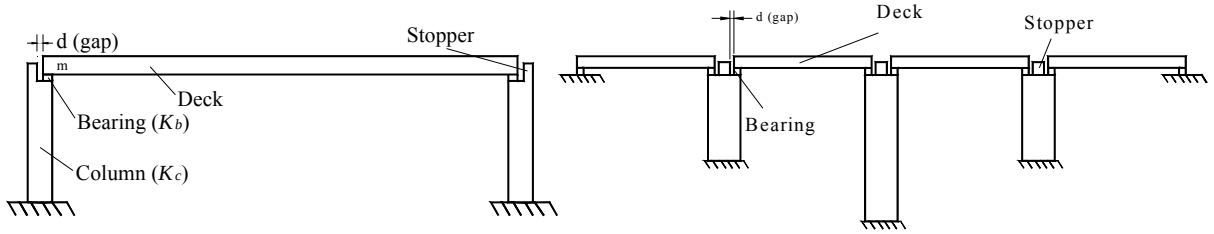

Figure 1: Schematic diagram of (a) single span bridge and (b) Kavala bridge.

In order to gain useful insight into the behavior of these systems, the response characteristics of the SDOF piecewise linear elastic systems, shown in Figure 2b, are first analyzed and the behavior to short duration sine pulses as well as longer duration transient excitations is investigated. The analysis is then extended to nonlinear systems possessing combined piecewise linear elastic and elasto-plastic restoring force characteristics. The analysis is concentrated on deterministic and probabilistic response spectra characteristics and the estimation of the sensitivity of these spectra to system and loading parameters, such as stiffness ratio, size of gaps, inelastic parameters, excitation strength and frequency content. It is shown that the performance of such systems to transient excitation can be enhanced by optimally designing the system parameter values. Issues related to the computational efficiency of the subset simulation method [6] and the two-stage subset simulation method [7] for computing the probabilistic response spectra are addressed. The analysis is then extended to investigate the response

and reliability of the four-span Kavala bridge (Figure 1b), located in northern Greece, under deterministic short duration sine pulse excitations as well as white noise stochastic excitations. The sensitivity of the response to the size of gaps is explored.

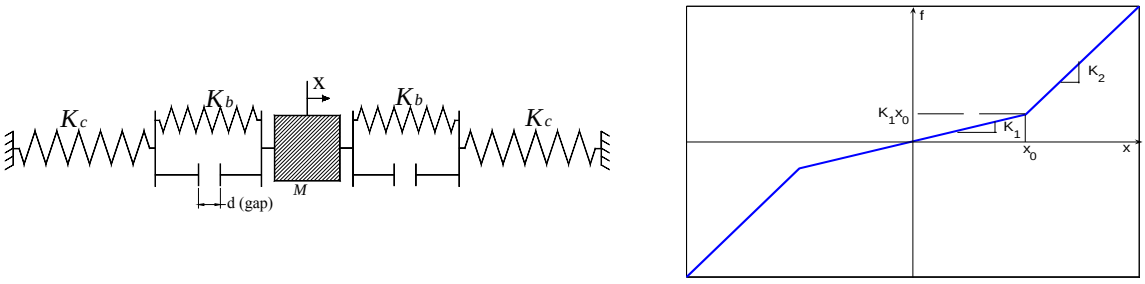

Figure 2: (a) Simplified SDOF system with bilinear stiffness and (b) elastic force-displacement relationship.

2 SDOF SYSTEM DESCRIPTION

2.1 Elastic system with gap elements

Consider in Figure 2a the SDOF model of the structure, shown in Figure 1a, with mass M, column stiffness K_c, bearing stiffness K_b and base excitation $\ddot{z}(t)$, assumed same at both left and right supports. The equation of motion for the model is given by

$$M\ddot{x} + C\dot{x} + f(x) = -M\ddot{z} \tag{1}$$

where the term $C\dot{x}$ accounts for the overall viscous damping on the system. The bilinear restore force due to the gap d is given by

$$f(x) = \begin{cases} K_1 \cdot x & -x_0 \le x \le x_0 \\ K_1 \cdot x_0 + K_2(x - x_0) & x > x_0 \\ -K_1 \cdot x_0 + K_2(x + x_0) & x < -x_0 \end{cases} \tag{2}$$

where $K_1 = 2K_c/(1+\kappa)$ is the stiffness of the system before impact, and $K_2 = K_1/(1+\kappa/2)$ is the stiffness of the system after impact, and $x_0 = d(1+\kappa)/\kappa$ is the mass displacement at which impact occurs, where $\kappa = K_c / K_b$ is the column to bearing stiffness ratio. By introducing the following non dimensional parameters:

$$\eta_1 = \frac{\omega_1}{\omega},\ x_N = \frac{a_g}{\omega^2},\ y(\tau) = \frac{x(t/\omega)}{x_N},\ y_0 = \frac{x_0}{x_N},\ \delta = \frac{d}{x_N},\ \tau = t \cdot \omega,\ p^*(\tau) = \frac{\ddot{z}}{a_g} \tag{3}$$

where $\omega_1 = \sqrt{\mathrm{K}_1 / \mathrm{M}}$ is the initial natural frequency of the SDOF before impact, ω and a_g is a characteristic frequency and amplitude of the excitation, respectively, and x_N is a characteristic displacement, the equation of motion becomes:

$$y'' + 2\zeta\eta_1 y' + \eta_1^2 F(y) = -p^*(\tau) \tag{4}$$

The non-dimensional column force defined by $f_c = F_c/(x_N M\omega^2)$, can be shown to be given by

$$f_c = y_c \eta_1^2 (1+\kappa)/2 \tag{5}$$

where $\bar{y}_c = \delta_c / x_N$ is the non-dimensional deflection (elongation) of the column spring, which can be shown to be given with respect to y as

$$\bar{y}_c = \begin{cases} \dfrac{y}{(\kappa+1)} & -y_0 \le y \le y_0 \\ y - \dfrac{\kappa}{1+\kappa} y_0 & y < -y_0, y > y_0 \end{cases} \tag{6}$$

The non-dimensional restoring force in (4) is given by

$$F(y) = \frac{1}{M \cdot x_N} f(y) = \begin{cases} y & -y_0 \le y \le y_0 \\ y_0 + \dfrac{2+\kappa}{2} \cdot (y - y_0) & y > y_0 \\ -y_0 + \dfrac{2+\kappa}{2} \cdot (y + y_0) & y < -y_0 \end{cases} \tag{7}$$

2.2 Inelastic system with gap elements

In this case, the column springs are assumed to behave as elastic perfectly plastic elements with yield displacement x_{yield} and yield force F_{yield}. The equation of motion for the system is given by (1) with the force $F(y)$ depending on the restoring force characteristics of the column spring. Due to the elastoplastic behaviour of the column springs, the force-displacement relationship of the equivalent piecewise-linear inelastic spring of the SDOF system is shown in Figure 3a. Figure 3b gives the force-displacement hysteretic loop computed using a harmonic excitation. Note that x_0 denotes the mass displacement at impact, x_1 is the mass displacement at the first yield of the column spring and x_2 is the mass displacement at the second yield of the other column spring.

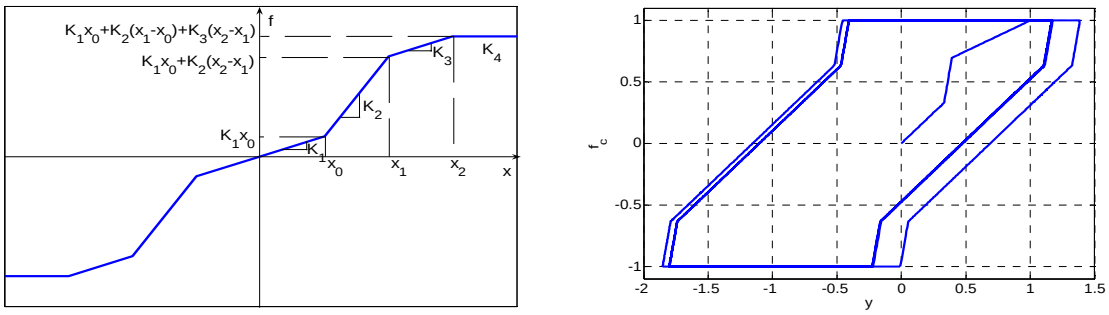

Figure 3: (a) Elastic force-displacement relationship and (b) hysteretic loop.

By introducing the non dimensional parameters (3), along with the non-dimensional mass displacement $y_1 = x_1 / x_N$ corresponding to the position of yield of the first column spring and the non-dimensional mass displacement $y_2 = x_2 / x_N$ corresponding to the position of yield of the second column spring, the equation of motion is given by (4), where $F(y)$ is a piecewise linear restoring force derived from $f(x)$ given in Figure 3. The non-dimensional yield displacement and yield force of the column spring is $y_{yield} = x_{yield} / x_N$ and $f_{yield} = F_{yield} / (a_g M)$, respectively. The ductility of the column is defined by

$$\mu_c = \frac{x_c}{x_{yield}} = \frac{y_c}{y_{yield}} \tag{8}$$

where x_c (y_c) is the deflection (normalized deflection) of the top of the column or, equivalently, the elongation of the column spring, and x_{yield} (y_{yield}) is the respective yield deflection (normalized deflection) of the top of the column. The ductility of the system is defined by

$$\mu_s = \frac{x}{x_1} = \frac{y}{y_1}, \tag{9}$$

where x_1 (y_1) is the displacement (normalized displacement) of the mass at the position of first yield.

3 RESPONSE TO PULSE EXCITATION

The characteristics of the response of the structure to pulse excitation, representing near field earthquake excitations, are first considered. A sine pulse excitation of the form

$$\ddot{z} = \begin{cases} a_g \sin \omega t, & t \le \mathrm{T} = \dfrac{2\pi}{\omega} \\ 0, & t > \mathrm{T} \end{cases} \tag{10}$$

is assumed. The normalized pulse load $p^*(\tau)$, defined in (3), is given by

$$p^*(\tau) = \begin{cases} \sin \tau, & \tau \le 1 \\ 0, & \tau > 1 \end{cases} \tag{11}$$

Parametric plots of the response of the elastic and inelastic SDOF systems are presented in Figures 4 and 5 for constant damping coefficient $\zeta = 5\%$ and stiffness ratio $\kappa = K_c / K_b = 10$. Specifically in Figures 4a and b are presented the response spectra of the mass displacement for the elastic and inelastic system respectively, versus the non-dimensional period $\eta_1 = \omega_1 / \omega = T / T_1$ and for different values of the non-dimensional gap length δ. For the elastic system it is shown that the displacement of the mass is decreasing with respect to η_1 for given δ, whereas it is increasing with respect to δ for given η_1. Next, in Figures 5a and b are presented the column force spectra for the elastic system and the column ductility spectra for the inelastic system, respectively, versus the non-dimensional period η_1 and for different values of the non-dimensional gap length δ. The inelastic spectra correspond to non-dimensional yield force $f_{yield} = 0.5$. For this value of yield force the mass of the system first impacts the stopper before the yielding of the column. It is shown that the force spectra for the elastic system exhibit complex behavior and that the maximum force for each δ appears to be in different values of the normalized excitation frequency η_1.

For the cases of non dimensional gap lengths $\delta \to \infty$ or $\delta \to 0$, the system responds linearly. In the case of $\delta \to \infty$ no impact occurs during the motion and the system corresponds, due to symmetry, to a linear SDOF system with natural frequency ω_1. In the second case of $\delta \to 0$ the system also corresponds, due to symmetry, to a linear SDOF system with mass M and with equivalent stiffness composed from the stiffness of three springs, the spring that consists of a K_c spring on one side of the system connected in parallel with the group of the

two springs (K_c and K_b) connected in series on the other side. The natural frequency of the SDOF system is $\omega_2 = \omega_1\sqrt{(2+\kappa)/2} > \omega_1$.

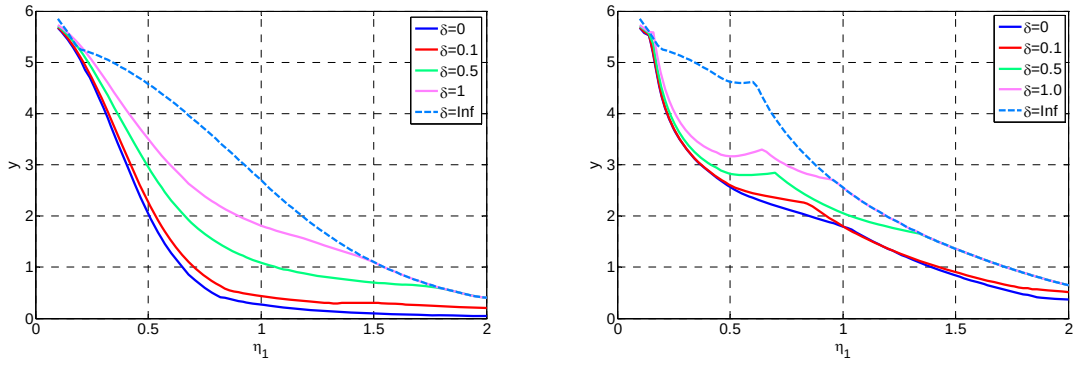

Figure 4: Mass displacement for (a) elastic system and (b) inelastic system.

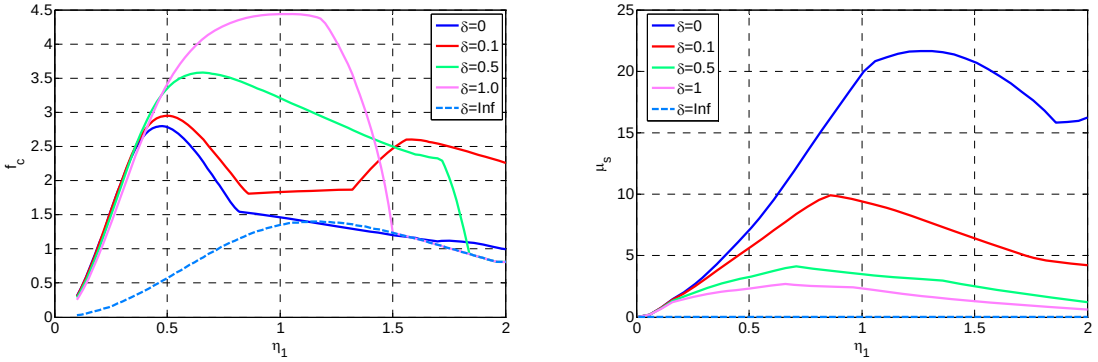

Figure 5: (a) Column forces for elastic system and (b) ductility of inelastic system.

Thus, the linear system $\delta \to 0$ has lower period $T_2 < T_1$ than the linear system with $\delta \to \infty$. This clearly shows in the elastic response spectra since the period of excitation for which the peak response occurs shifts from $\eta_1 \approx 1$ to lower values close to $\eta_1 \approx T_2 / T_1$. For intermediate values δ, the maximum response in the nonlinear elastic response spectra occurs between the value of $\eta_1 \approx 1$ and $\eta_1 \approx T_2 / T_1$. In particular as the value of δ reduces from $\delta \to \infty$ to $\delta \to 0$, the system period reduces since the reduction of the gap δ tends to increase the stiffness of the elastic system and, as a result, the peak in the response spectra moves to the left towards smaller values of η_1. For the inelastic system the opposite trend is true which is due to the fact that the equivalent period of the inelastic system, for a given value of the frequency ω_1 of the linear system tends to increase as the value of δ reduces. This increase is caused by the softening behavior the column elastoplastic elements which dominates the hardening behavior of the nonlinear elastic system for the chosen value of the ultimate resistant load f_y for the elastoplastic column elements.

It is worth noting that the intermediate values of the gap δ amplifies by two or three times the normalized forces in the linear columns in relation to the forces for the linear systems $\delta \to 0$ and $\delta \to \infty$. In contrast, the displacement response spectra of the mass for these intermediate values of δ are contained within the displacement response spectra for the two linear systems $\delta \to 0$ and $\delta \to \infty$. Comparing the displacement spectra in Figure 4 for the elastic and inelastic system, it is observed that the displacements of the inelastic system are

amplified close to resonance in relation to displacements for the elastic system. As it is clearly seen in Figure 4, for relatively high values of the excitation period T or η_1, which depend on the δ values, the nonlinearities (elastic and inelastic) are not activated and thus the system behave linearly.

Next in Figures 6 and 7 are shown the mass displacement, column force and system ductility spectra versus the non-dimensional gap length δ for different values of the non-dimensional system period η_1, for the elastic and inelastic systems. The mass displacement for both systems increases as δ increases, until it reaches a high enough value beyond which there is no impact and the system responds linearly. Note that the straight line, given by $y = \delta(1+\kappa)/\kappa$, that appears in Figure 6 and 7 divides the spectra in two areas. The left area is the one that at least one impact has occurred and therefore the system responds non-linearly. That is the non dimensional gap length is small enough so that there is at least one impact for each value of δ and η_1. When the value of the non dimensional gap length is not small enough for impact to occur, the systems responds linearly and therefore there is no change in the response amplitude as the value of δ increases.

For the column force spectra it is shown that these forces are always greater when at least one impact has occurred, while the maximum column force appears for different δ. The influence of the non-dimensional gap length δ is also seen in these figures since it effects the stiffening or softening behavior of the system. Specifically as the non-dimensional gap length decreases, the "equivalent linear" stiffness of the system increases and so does the "equivalent linear" natural frequency. This results in resonance phenomena appearing for smaller values of the non-dimensional excitation period η_1 corresponding to smaller values of the non-dimensional gap length.

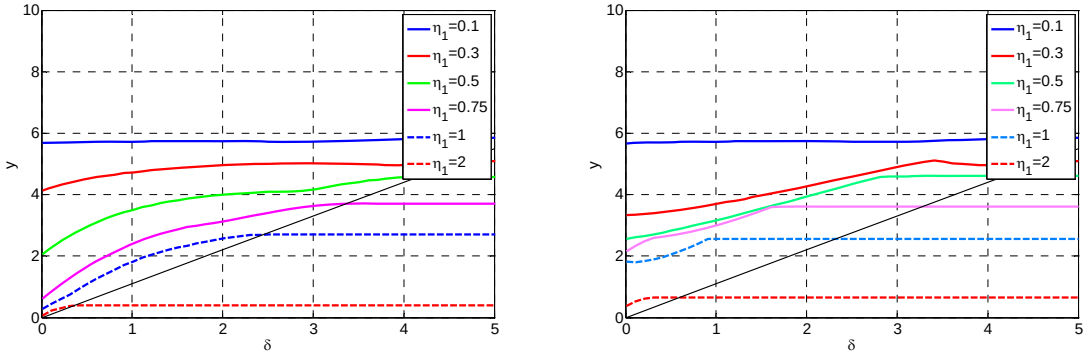

Figure 6: Mass displacement for (a) elastic system and (b) inelastic system.

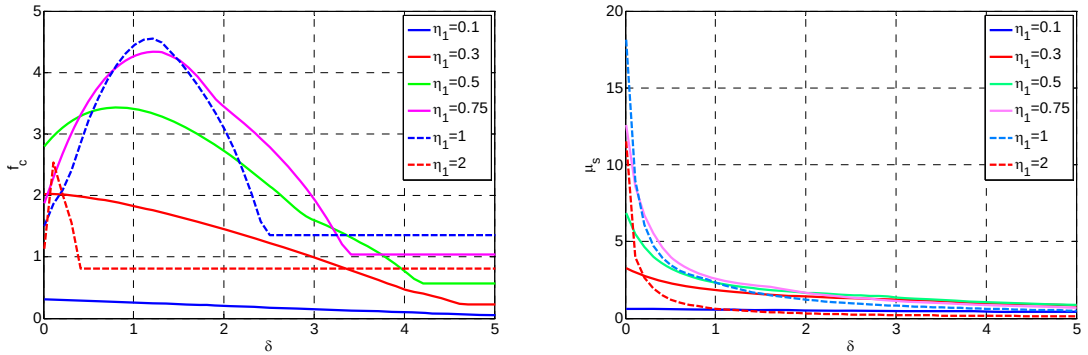

Figure 7: (a) Column forces for elastic system and (b) ductility of inelastic system.

4 RESPONSE TO RECORDED EARTHQUAKE EXCITATION

The response spectra of the system to recorded earthquake excitation are next obtained. The base acceleration recorded at Sepolia (Athens) metro station during the 1999 Ano Liosia (Athens) earthquake of magnitude 6 Richter is used as the excitation. The characteristic input frequency was chosen to be $\omega = 4.22\,(2\pi)$ rad/sec and the value of $x_N = a_g / \omega^2 = 0.14$ was based on $a_g = \ddot{z}_{\max}$.

Response spectra of the mass displacement and column force for the elastic and inelastic system are presented in Figures 8 and 9 as a function of η_1 for different values of δ and in Figures 10 and 11 as a function of δ for different values of η_1. These figures should be compared to Figures 4 to 7 for pulse excitation. It can be seen that the maximum response (displacement, force or ductility) appears to occur for different values of η_1 which depend on the values of δ that controls the hardening or softening behavior of the elastic and inelastic systems. The results observed for the earthquake excitation are similar to, in some respect, those obtained for the sine pulse excitation.

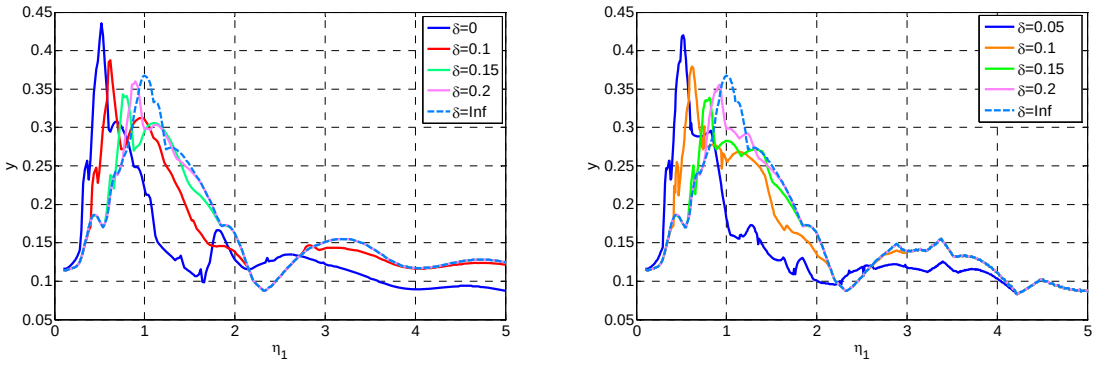

Figure 8: Mass displacement for (a) elastic system and (b) inelastic system.

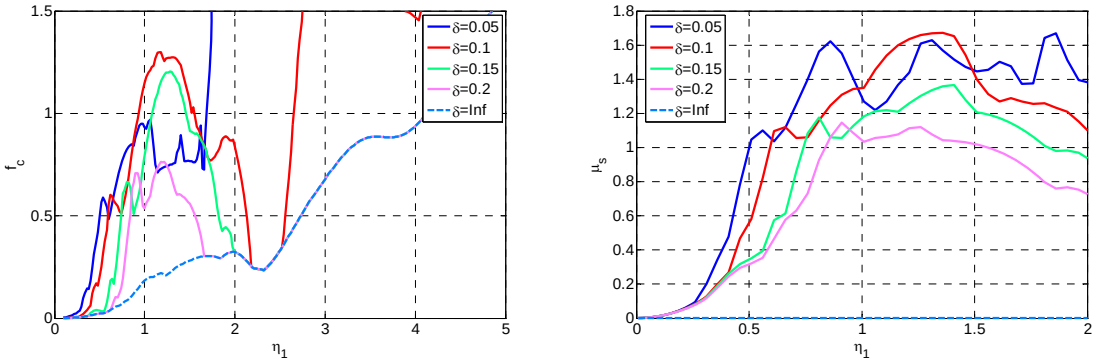

Figure 9: (a) Column forces for elastic system and (b) ductility of inelastic system.

5 RELIABILITY ANALYSIS

The response to a white noise stochastic base excitation is next considered. The levels b with fixed probability of not been exceeded by the response are obtained. These levels as a function of one of the systems parameters such as η_1 or δ represent the probabilistic response spectra. In Figures 12 and 13 is shown the behavior of the probabilistic elastic and inelastic displacement response spectra that have 10^{-3} probability to be exceeded as a function of the system parameters η_1 and δ. For the calculation of the probabilistic response spectra, corre-

sponding to fixed failure probability, the subset simulation method [6] is used for 500 samples for computing the intermediate 10^{-1} failure levels.

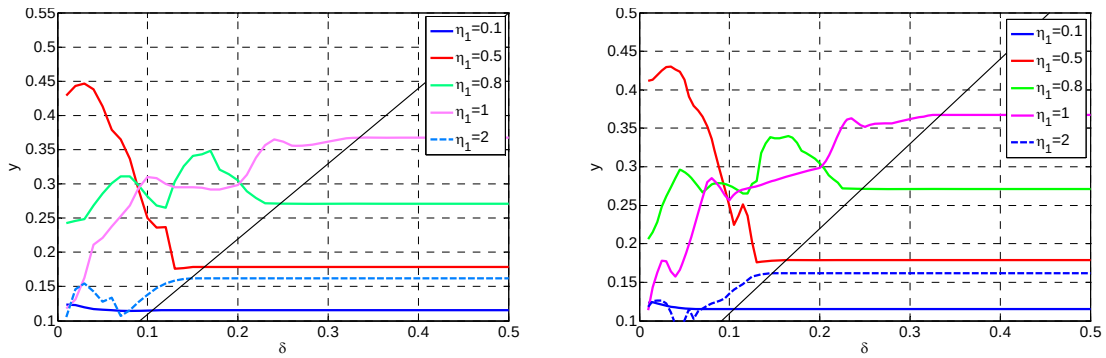

Figure 10: Mass displacement for (a) elastic system and (b) inelastic system.

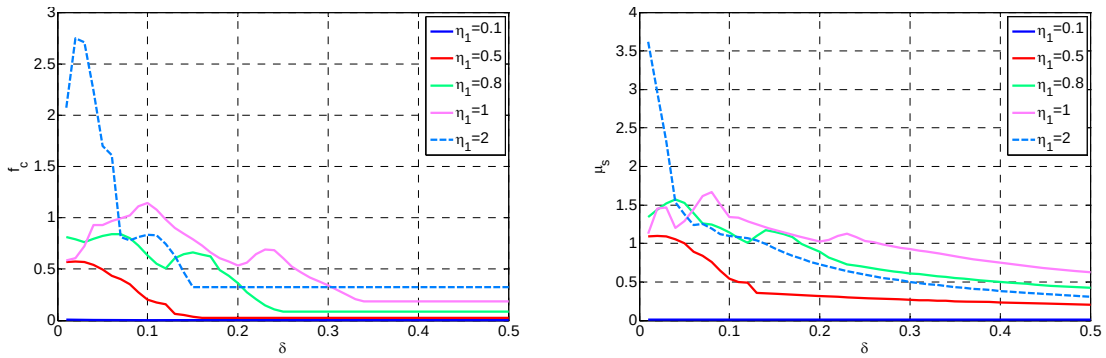

Figure 11: (a) Column forces for elastic system and (b) ductility of inelastic system.

The probabilistic response spectra for the mass displacement, corresponding to a fixed failure probability, show a very similar behavior to the mass response spectra obtained for the pulse excitation in Figures 4 and 6. The normalized period of excitation η_1 at which resonance occurs depends on the gap value δ. For the elastic system, as the gap reduces from $\delta \to \infty$ to $\delta = 0$ values, the system shows a hardening behavior and the peak of the probabilistic response spectra moves to the left from $\eta_1 \approx 1$ to $\eta_1 = T_2 / T_1$ values. For the inelastic system the resonance peak is affected by the softening behavior of the column elastoplastic elements which can dominate the hardening effect caused by the impact.

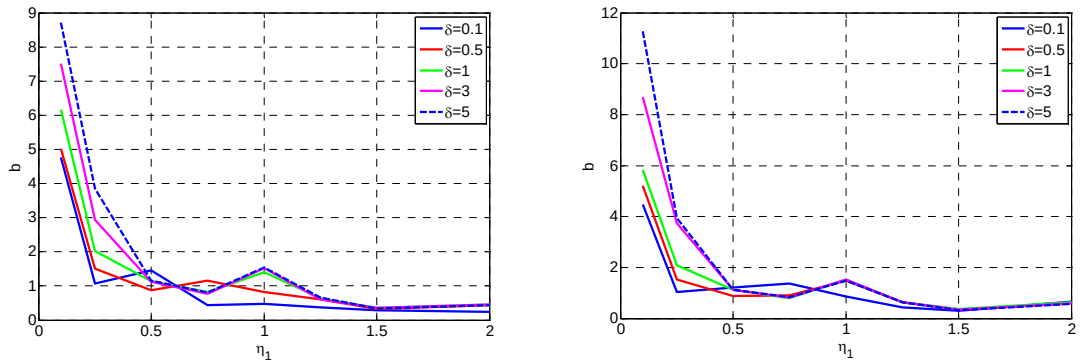

Figure 12: Mass displacement levels for 10^{-3} failure probability versus non-dimensional period for (a) elastic system and (b) inelastic system.

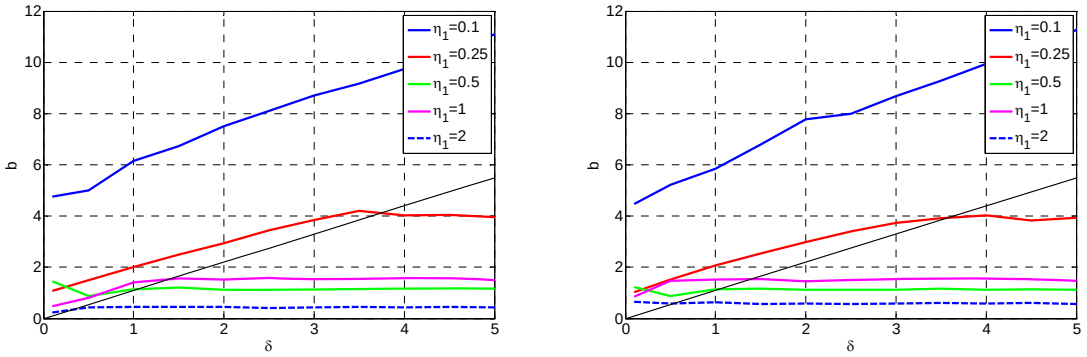

Figure 13: Mass displacement levels for 10^{-3} failure probability versus non-dimensional gap length for (a) elastic system and (b) inelastic system.

Next, a comparison between subset simulation method and the two stage subset simulation method for bilinear systems [7] is presented in order to investigate the efficiency of these two method for this specific non linear system. The probabilities of failure as a function of exceedance levels for the mass displacement of the elastic system are given in Figure 14 for the two methods, using 500 samples for computing the 10^{-1} intermediate failure levels, and for several runs of the two algorithms. Besides the smallest computational effort required by the two stage subset simulation method, its accuracy seems to be better for these type of systems, as it can be inferred by comparing the scatter of the multiple simulation curves.

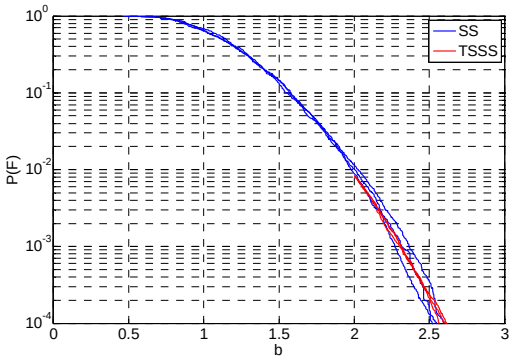

Figure 14: Comparison between subset simulation (SS) and two stage subset simulation (TSSS).

6 RESPONSE AND RELIABILITY OF KAVALA BRIDGE

The methodology is used to investigate the response and reliability of the four-span Kavala bridge [8], located in northern Greece, under earthquake excitations. A schematic diagram of the bridge is shown in Figure 1b. The bridge deck is supported on columns through elastomeric bearings. The bridge system involves piecewise linear stiffness elements that arise from impacts between the deck and the columns during moderate to strong earthquake shaking, while the columns of the bridge are allowed to behave inelastically. A multi degree of freedom finite element models of the bridge, involving inelastic elements and piecewise linear stiffness elements, is used to simulate its behavior. In order to have a better insight of the effect of such non linearities, a 2-D model of the four-span Kavala bridge is constructed. An 18 degrees of freedom finite element model is constructed using one beam element for each spam and column, as well as spring elements to model the stiffness of the elastomeric bearings.

Deterministic short duration sine pulse excitations, given in (10), as well as white noise stochastic excitations are used to simulate the short and moderate duration earthquake excita-

tions. The vulnerability of such bridge structure to these types of earthquake excitations is explored. Finite element analysis software OpenSEES [9] is used to perform the deterministic and stochastic dynamic analysis.

The elastic displacement response spectra to sine pulse base excitation are shown in Figure 15a as function of the frequency ω of the pulse for fixed values of the normalized gap δ and in Figure 15b as a function of the gap δ for fixed values of the pulse frequency ω. It is clear from the Figure 15a that the structure hardens as the gap value reduces from $\delta \to \infty$ to lower values. This behavior is evident by the shift of the peak value towards the right of the deck displacement spectra. In Figure 15b the displacement spectra are shown an irregular behavior that depends on the gap value δ and the frequency ω of the excitation.

The probabilistic response spectra of the normalized deck displacement and the left pier force to white noise base excitation are shown in Figures 16a and 16b as a function of the normalized gap δ. The behavior of the probabilistic response spectra levels for the deck displacement corresponding to fixed failure probability levels of 10^{-1}, 10^{-2} and10^{-3} is similar to the behavior of the deterministic response spectra curves for the deck displacement shown in Figures 15b for the pulse excitation The column forces increase for intermediate values of the normalized gap δ.

7 CONCLUSIONS

Single degree of freedom mechanical systems with piecewise linear elastic and elastoplastic behavior exhibit complex nonlinear behavior when subjected to transient and stochastic excitations. It is shown that the performance of piecewise linear elastic and inelastic SDOF systems to transient excitation, such as short sine pulse, earthquake-like and stochastic excitations, depends, among other system parameters, on the gap sizes which affect the deterministic and probabilistic response spectra. Studies on multi-degree-of-freedom model of a four-span Kavala bridge also show that the response spectra are affected by the size of the gap between the deck structure and the seismic stoppers of the pier cap. The design of the gap is critical in assessing the behavior of the bridge under transient earthquake excitation. The response and reliability characteristics of such systems can be enhanced by optimally designing the system parameter values. The proposed analysis framework is useful for investigating the vulnerability of such bridge systems to earthquake excitations.

ACKNOWLEDGEMENTS

This research was funded by the General Secretariat of Research and Technology (Greek Ministry of Development) and the European Research Fund, through the EPAN program framework under grant DP15. This support is gratefully acknowledged.

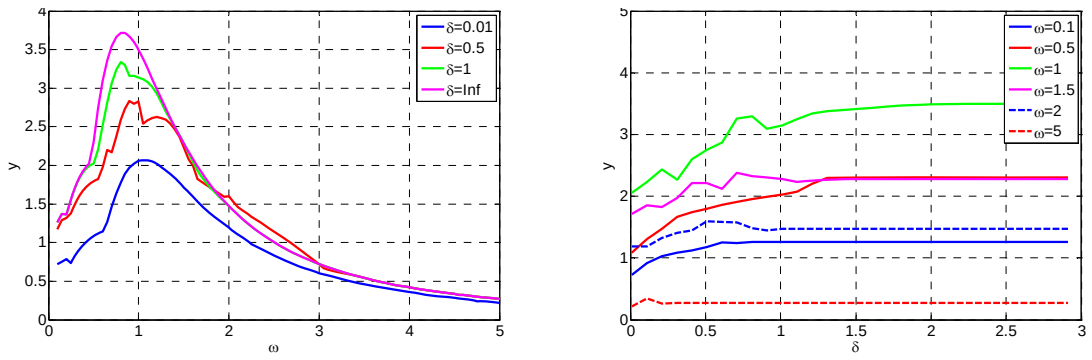

Figure 15: Deck displacement (a) as a function of ω for given δ and (b) as a function of δ for given ω.

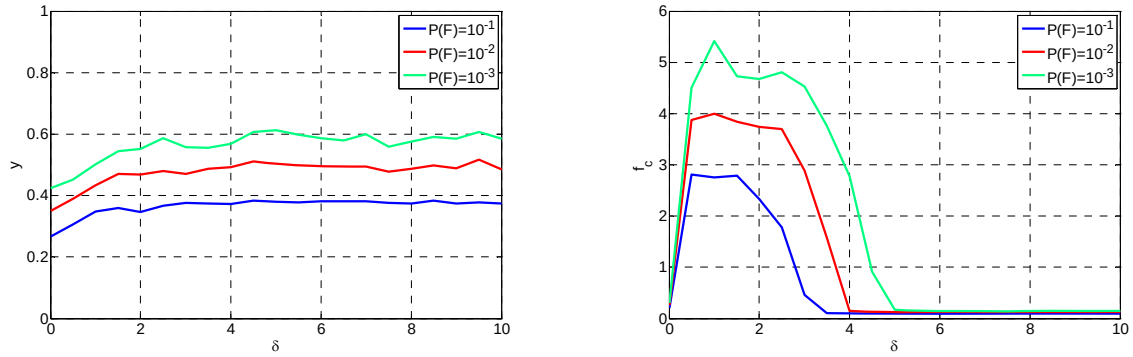

Figure 16: (a) Deck displacement and (b) column force for different failure levels.

REFERENCES

[1] S. Natsiavas, H. Gonzalez, Vibration of harmonically excited oscillators with asymmetric constrains. *Applied Mechanics*, **59**, 284-290, 1992.

[2] S. Natsiavas, Periodic response and stability of oscillators with symmetric trillinear restoring force. *Sound and Vibration*, **134**, 315-331, 1989.

[3] I.N. Psycharis, G.E. Mageirou, Investigation if the nonlinear response of bridges with elastomeric bearings and seismic stoppers. A simplified method of analysis. *Technical Chronics of Science*, **2-3**, 155-171, 2004.

[4] S. Maleki, Effect of side retainers on seismic response of bridges with elastomeric bearings. *Bridge Engineering*, **9**, 95-100, 2004.

[5] S. Maleki, Seismic modelling of skewed bridges with elastomeric bearings and side retainers. *Bridge engineering*, **10**, 442-449, 2005.

[6] S.K. Au, J.L. Beck, Estimation of small failure probabilities in high dimensions by subset simulation, *Probabilistic Engineering Mechanics,* **16**, 263-277, 2001.

[7] L. Katafygiotis, S.H. Cheung, A two-stage Subset Simulation-based approach for calculating the reliability of inelastic structural systems subjected to Gaussian random excitations. *Computer Methods in Applied Mechanics and Engineering*, **194**, 1581-1595, 2005.

[8] K. Christodoulou, Methodology for structural identification and damage detection, PhD Thesis Report SDL-06-01, Dept of Mechanical and Industrial Engineering, University of Thessaly, 2006.

[9] Open System for Earthquake Engineering Simulation (OpenSEES), http://opensees.berkeley.edu.